Hydrodynamic Relations for Direct-Drive Inertial Confinement Fusion Implosions

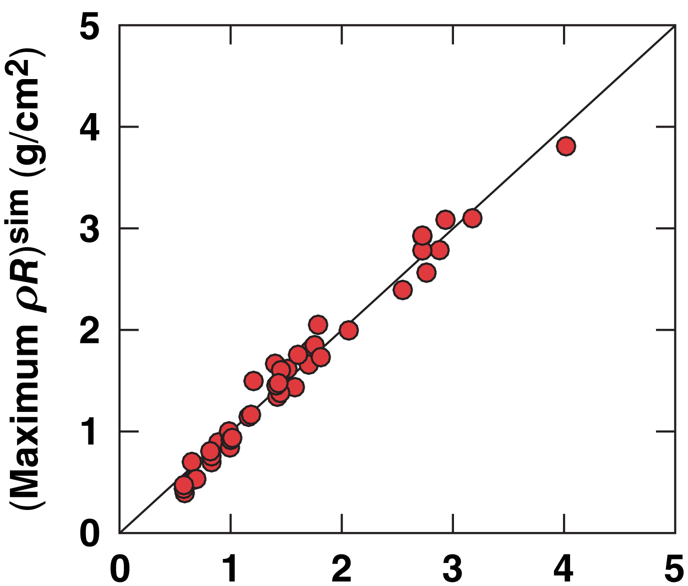

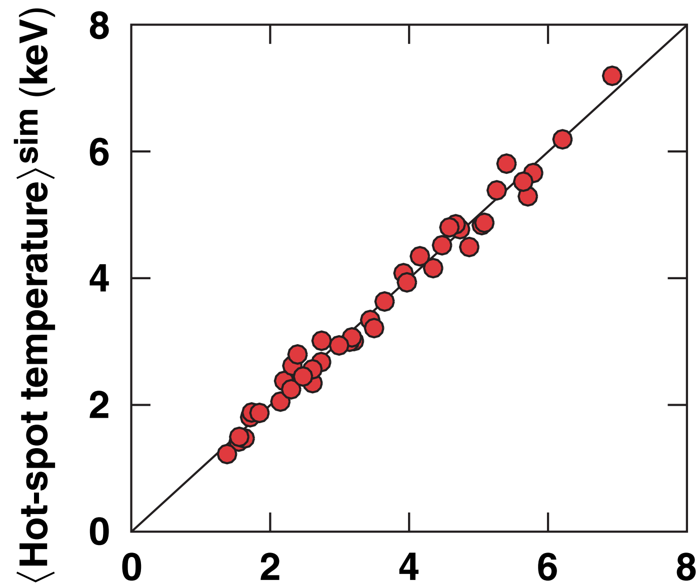

$$(\rho R)^{\mathrm{fit}}_{\mathrm{max}} = \frac{1.2}{\alpha_{\mathrm{in}}^{0.54}}\left[\frac{E_L\,(\mathrm{kJ})}{100}\right]^{0.33}\left[\frac{0.35}{\lambda_L\,(\mu\mathrm{m})}\right]^{0.25}\left[\frac{V_i\,(\mathrm{cm/s})}{3\times10^{7}}\right]^{0.06}$$

$$\langle T\rangle^{\mathrm{fit}}_{\mathrm{hs}} = \frac{3.0}{\alpha_{\mathrm{in}}^{0.15}}\left[\frac{V_i\,(\mathrm{cm/s})}{3\times10^{7}}\right]^{1.25}\left[\frac{E_L\,(\mathrm{kJ})}{100}\right]^{0.07}$$

C. D. Zhou and R. Betti
University of Rochester
Fusion Science Center and
Laboratory for Laser Energetics

49th Annual Meeting of the
American Physical Society
Division of Plasma Physics
Orlando, FL
12–16 November 2007

Summary

Scaling laws relating stagnation and in-flight hydrodynamic variables are derived for the design of direct-drive ICF targets

- Such scaling laws can be used to optimize direct-drive target design.
- Scaling laws relating stagnation and in-flight variables are derived for hydrodynamic variables relevant to conventional and fast-ignition ICF
  - hydrodynamic efficiency and target gain
  - stagnation aspect ratio, shell density, and areal density
  - hot-spot areal density, temperature, and pressure
- Based on such scaling laws, fast-ignition targets require low-velocity, low-adiabat implosions

The simple rocket model yields the scaling of the hydrodynamic efficiency to be used in the gain formula

- Hydro-efficiency derived from the rocket model

$$\eta = \frac{\left(1 - \frac{M_a}{M_0}\right)\left[\ln\left(1 - \frac{M_a}{M_0}\right)\right]^2}{M_a/M_0}$$

- For $M_a < 0.7\ M_0$

$$\eta^{\text{theory}} \sim I_L^{-0.25}\, V_i^{0.75}\, \lambda_L^{-0.5}$$

  - I_L = laser intensity
  - V_i = implosion velocity
  - λ_L = laser wavelength

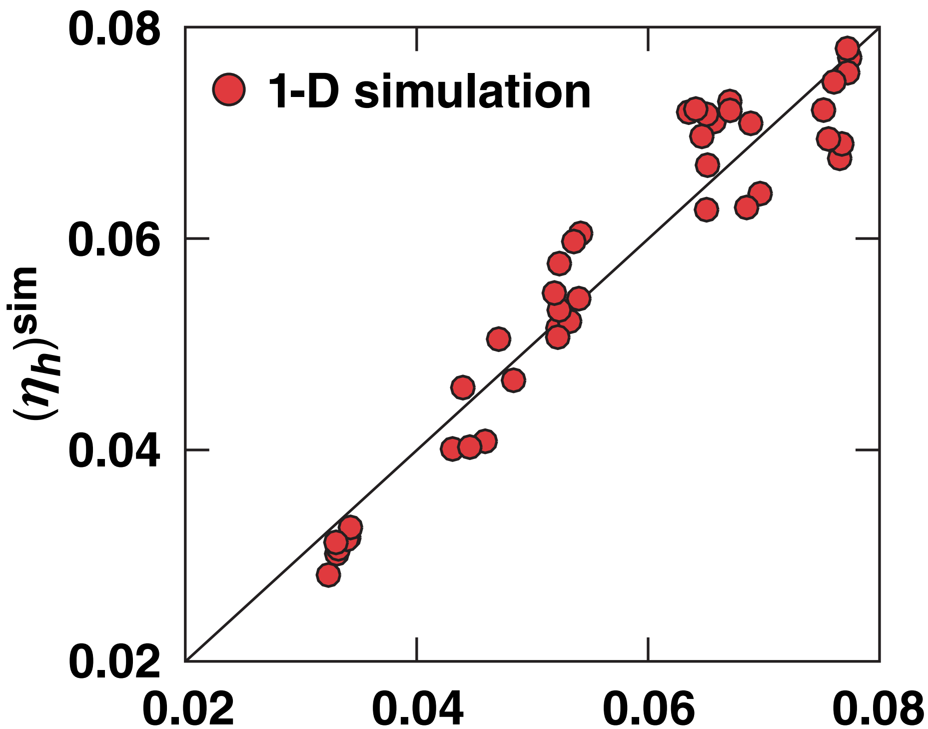

$$\eta^{\text{fit}} = \frac{0.051}{I_{15}^{0.25}}\left[\frac{V_i\,(\text{cm/s})}{3\times10^7}\right]^{0.75}\left[\frac{0.35}{\lambda_L\,(\mu\text{m})}\right]^{0.5}$$

TC7933

Energy gain increases for low-implosion velocity, high areal density, and shorter laser wavelength

$$G = \frac{E_{\text{Fusion}}}{E_{\text{Laser}}} = \frac{\theta E_f / m_{\text{ion}}}{V_i^2 / \eta} = \frac{\eta \theta E_f}{m_{\text{ion}} V_i^2}$$

$$\theta = \frac{1}{1 + 7 / \rho R \left(\text{g/cm}^2\right)} = \text{fraction burned}$$

M_{ion} = ion mass

E_f = 17.5 MeV

Gain formula

$$G = \frac{73}{I_{15}^{0.25}} \left[\frac{3 \times 10^7}{V_i \left(\text{cm/s}\right)}\right]^{1.25} \left(\frac{\theta}{0.2}\right) \left[\frac{0.35}{\lambda_L \left(\mu\text{m}\right)}\right]^{0.5}$$

- Higher ρR → longer burn time
- Lower V_i → more fuel mass for the same kinetic/laser energy

TC7934

In fast ignition, small hot spots require low-implosion velocity; the stagnation aspect ratio decreases with lower-implosion velocity

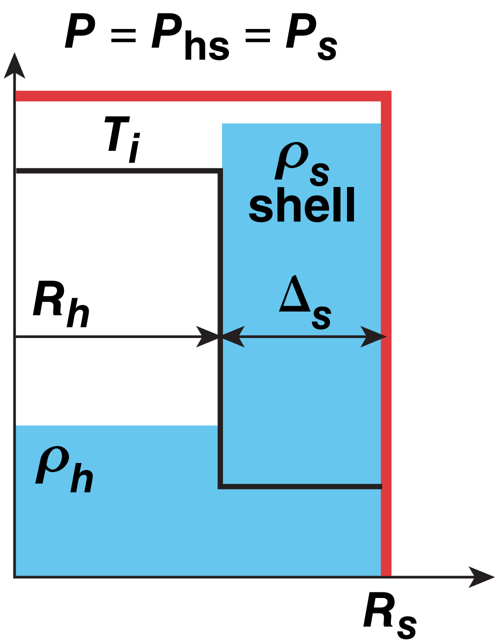

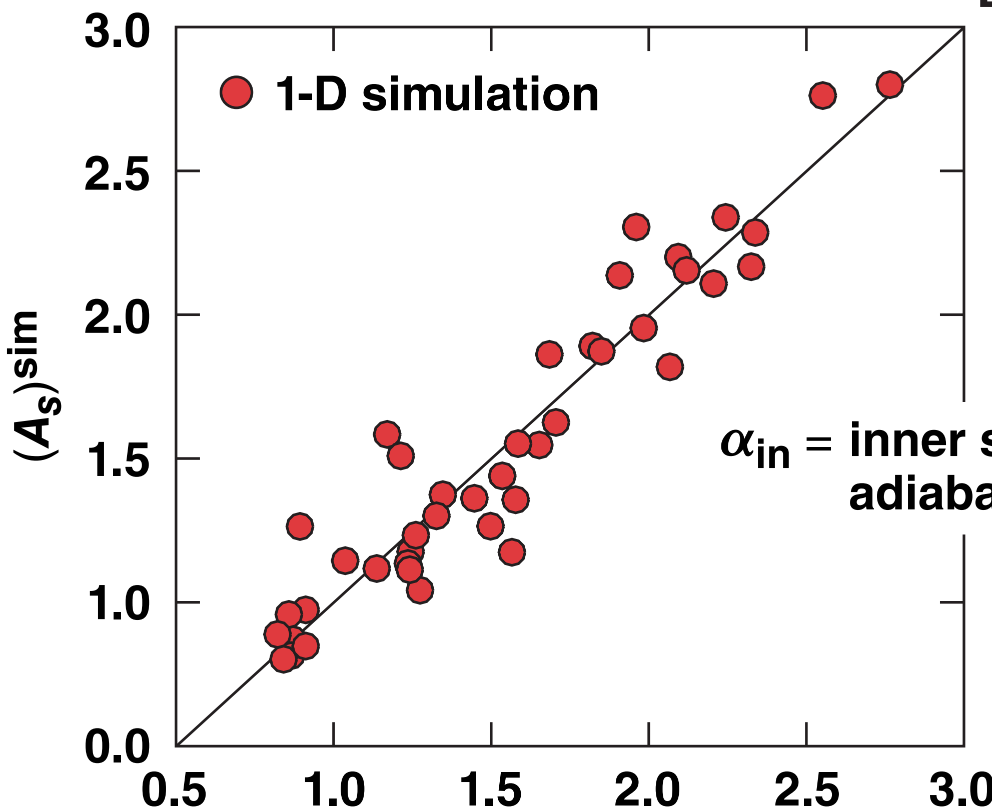

α_{in} = inner surface adiabat

Simulations are carried out for $1 < \alpha_{in} < 5$ and $2 \times 10^7 < V_i < 5.5 \times 10^7$ cm/s

$$A_s^{fit} \equiv \frac{R_h}{\Delta_s} \approx \frac{1.48}{\alpha_{in}^{0.19}} \left[\frac{V_i\,(\mathrm{cm/s})}{3 \times 10^7} \right]^{0.96}$$

TC7936

The shell areal density depends on adiabat and driver energy and is almost independent of implosion velocity

$$(\rho R)^{\text{theory}} \sim \alpha_{\text{if}}^{-0.63} E_L^{0.33} V_i^{0.03} \lambda_L^{-0.25}$$

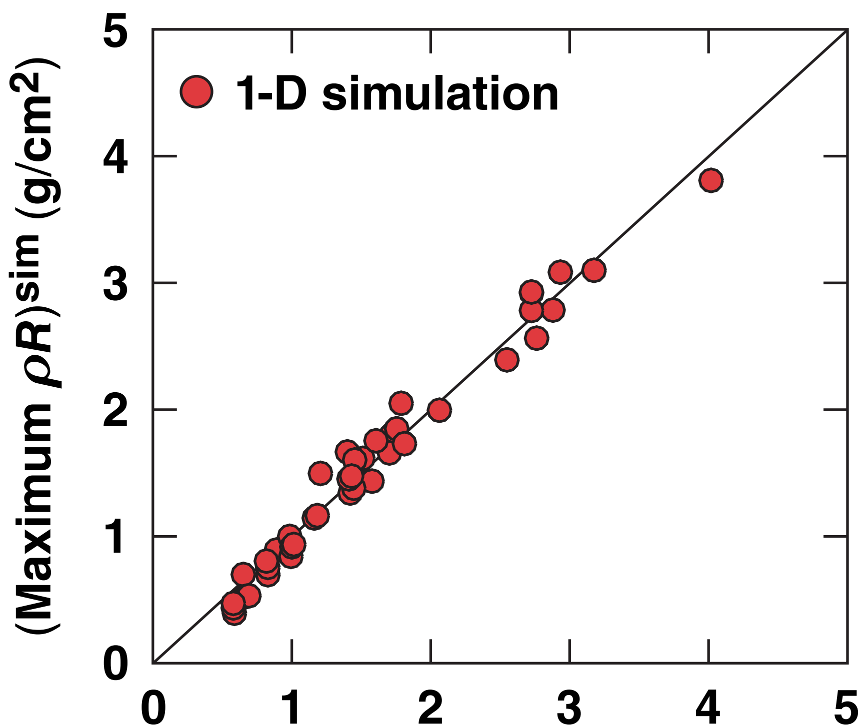

$$(\rho R)_{\text{max}}^{\text{fit}} = \frac{1.2}{\alpha_{\text{in}}^{0.54}} \left[\frac{E_L\,(\text{kJ})}{100}\right]^{0.33} \left[\frac{0.35}{\lambda_L\,(\mu\text{m})}\right]^{0.25} \left[\frac{V_i\,(\text{cm/s})}{3 \times 10^7}\right]^{0.06}$$

TC7937

The shell density depends on adiabat and implosion velocity and is independent of driver energy

FSC

UR LLE

$$\left(\rho\right)^{\text{theory}} \sim \alpha_{\text{if}}^{-1.08}\, V_i^{1.4}\, I_L^{0.13}\, \lambda_L^{-0.13}$$

Average density

$$\langle\rho\rangle_{\rho R} = \frac{\int \rho d\, \rho R}{\int d\, \rho R}$$

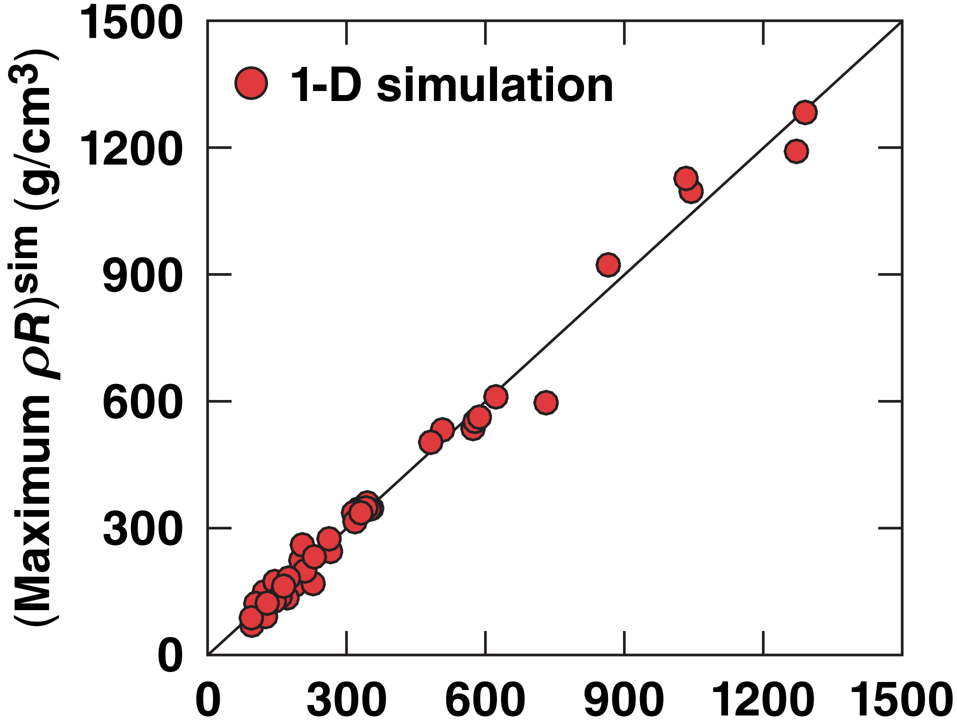

$$\langle\rho\rangle_{\rho R}^{\text{fit}} = \frac{425 \cdot I_{15}^{0.13}}{\alpha_{\text{in}}^{1.12}} \left[\frac{V_i\,(\text{cm/s})}{3\times 10^7}\right] \left[\frac{0.35}{\lambda_L\,(\mu\text{m})}\right]^{0.13}$$

TC7938

Stagnation hydro-properties derived from the hot-spot energy balance, the thin-shell equation of motion, and the hot-spot mass conservation

- Hot-spot energy equation

$$\frac{dE_h}{dt} + 3\,p_h R_h^2 \dot{R}_h = 0$$

$$E_h = \frac{3}{2} p_h R_h^3$$

- Hot-spot equation of motion

$$M_s \ddot{R}_h = 4\pi R_h^2 p_h$$

- Hot-spot mass conservation

$$\frac{dM_h}{dt} = 4\pi R_h^2 \dot{m}_a \qquad \dot{m}_a = \frac{12\,A\kappa_{\text{Spitzer}}(T)}{25\,R_h}$$

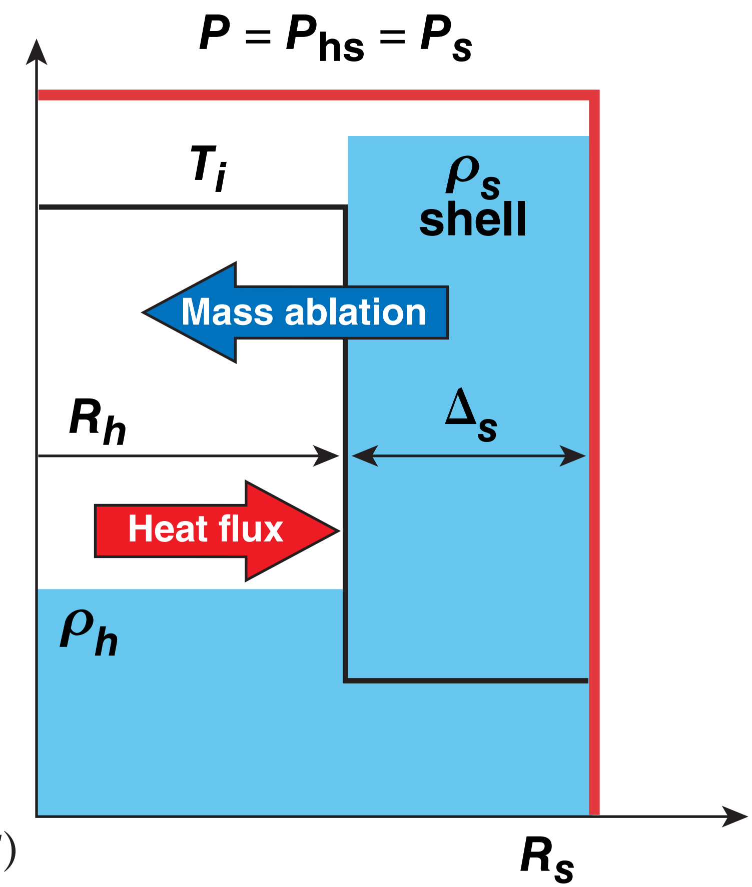

TC7939

The stagnation hot-spot pressure depends on implosion velocity and adiabat

$$\left(p_{hs}\right)^{theory} \sim \alpha_{if}^{-1.40} V_i^{3.02}$$

Pressure averaged over hot-spot volume

$$\langle p \rangle_{hs} = \frac{\int_0^{R_h} p\,dr^3}{R_h^3}$$

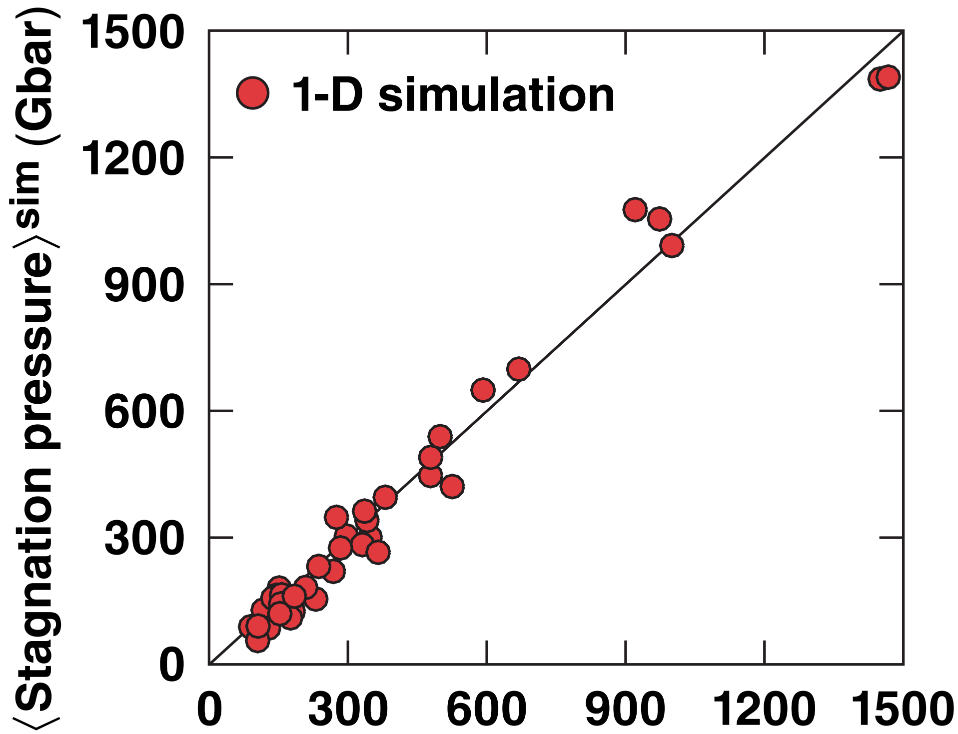

$$\langle p \rangle_{hs}^{fit} = \frac{345}{\alpha_{in}^{0.90}} \left[\frac{V_i\,(cm/s)}{3 \times 10^7}\right]^{1.85}$$

TC8028

The hot-spot temperature decreases with lower-implosion velocity

$$\left(T_{hs}\right)^{theory} \sim \alpha_{if}^{-0.23} V_i^{1.12} E_L^{0.09}$$

Ion temperature averaged over hot-spot volume

$$\langle T \rangle_{hs} = \frac{\int_0^{R_h} T dr^3}{R_h^3}$$

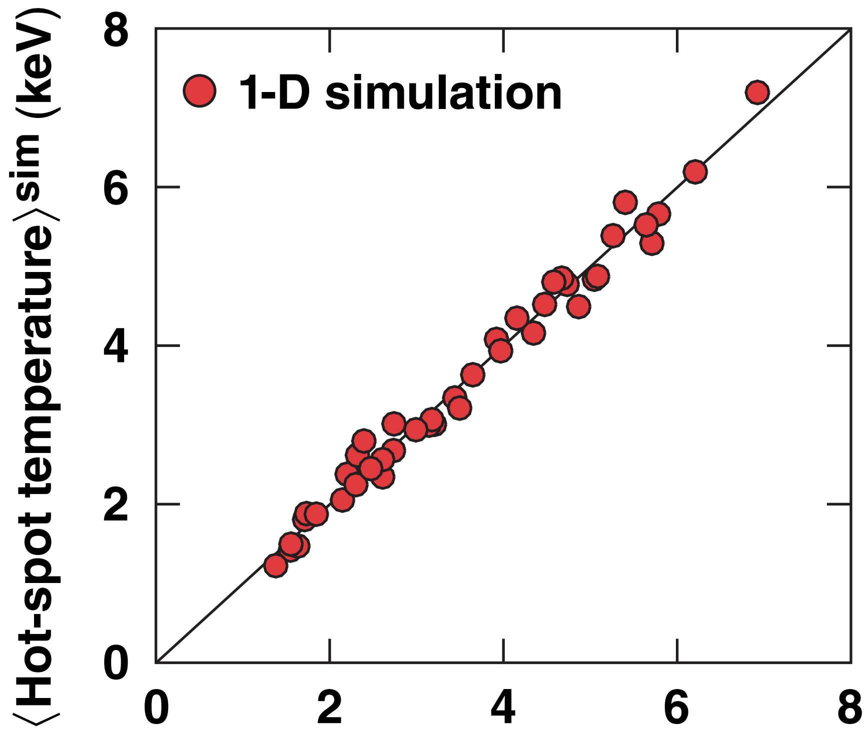

$$\langle T \rangle_{hs}^{fit} = \frac{3.0}{\alpha_{in}^{0.15}} \left[\frac{V_i\,(\mathrm{cm/s})}{3 \times 10^7}\right]^{1.25} \left[\frac{E_L\,(\mathrm{kJ})}{100}\right]^{0.07}$$

TC8029

The stagnation hot-spot areal density depends on adiabat, driver energy, and implosion velocity

$$\left(\rho R_{hs}\right)^{\text{theory}} \sim \alpha_{if}^{-0.49} V_i^{1.38} E_L^{0.24}$$

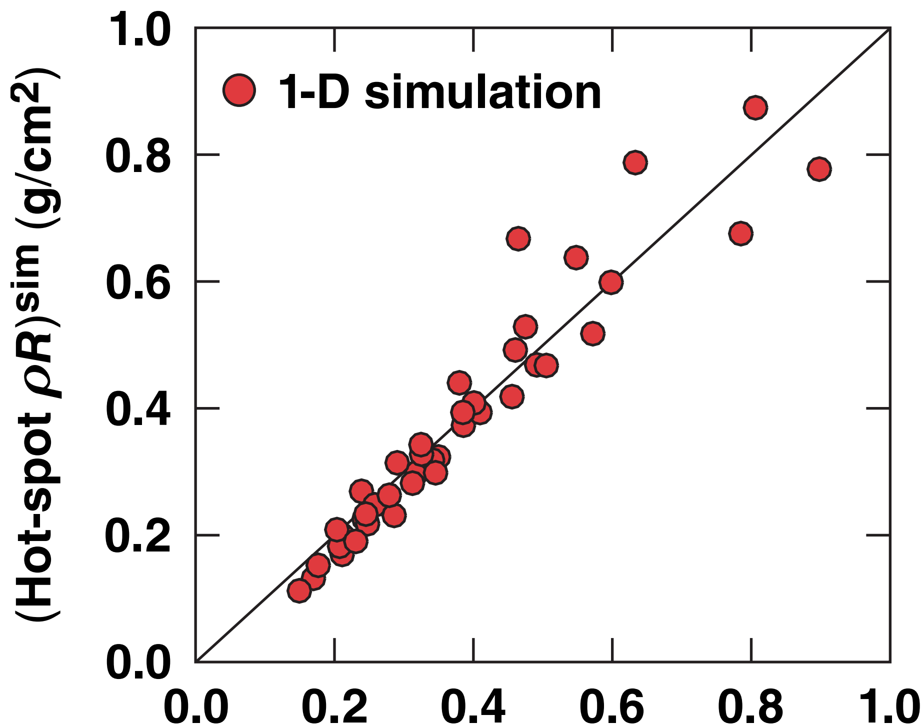

$$\langle \rho R \rangle_{hs}^{\text{fit}} = \frac{0.31}{\alpha_{in}^{0.55}} \left[\frac{V_i\,(\text{cm/s})}{3 \times 10^7}\right]^{0.62} \left[\frac{E_L\,(\text{kJ})}{100}\right]^{0.27}$$

$$\rho R_{hs} \approx 0.26\, \rho R_{\text{shell}} \left[\frac{V_i\,(\text{cm/s})}{3 \times 10^7}\right]^{0.62}$$

TC8030

Optimized fast-ignition cryo targets are thick shells of wetted foam with an initial aspect ratio of ~2

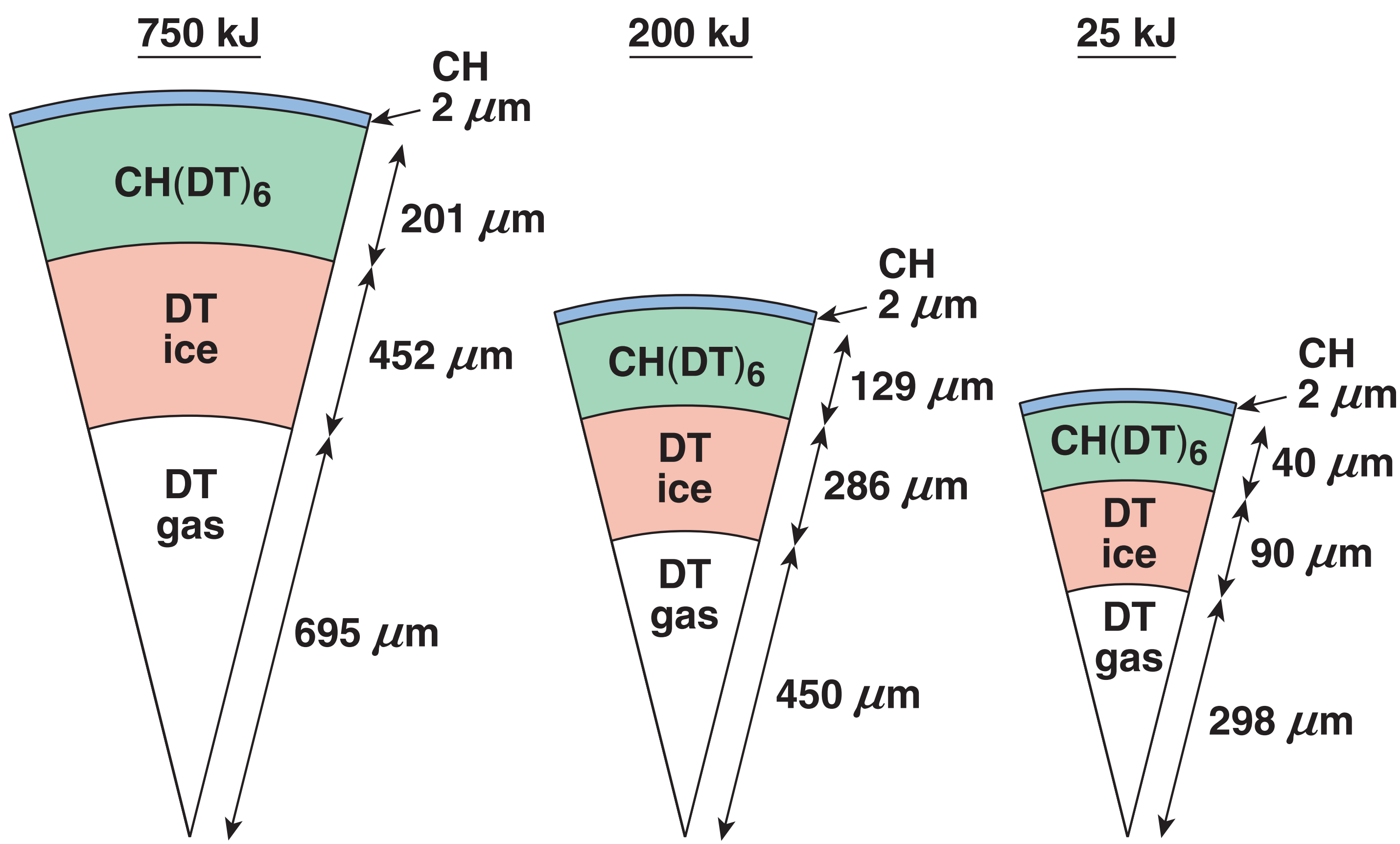

TC7585c

These targets have high areal densities and low IFAR

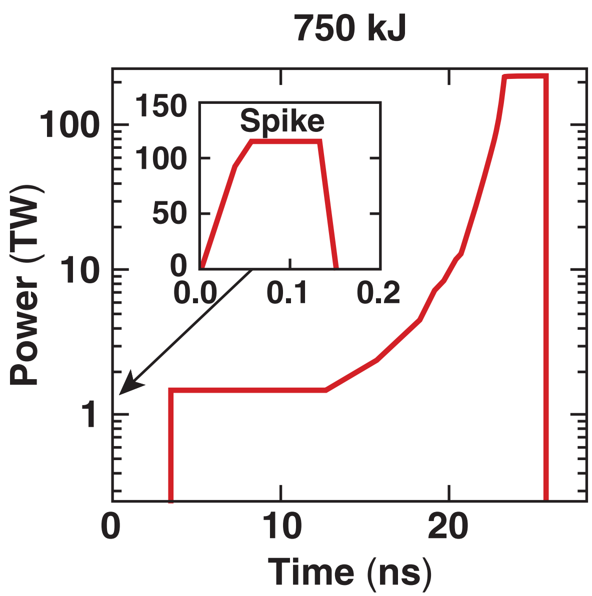

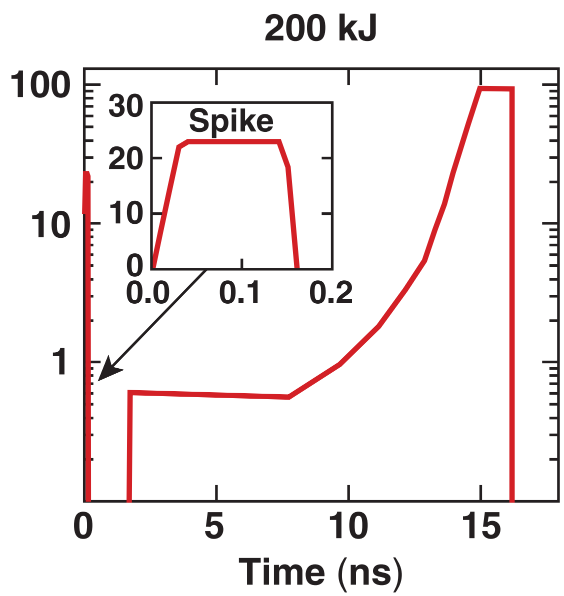

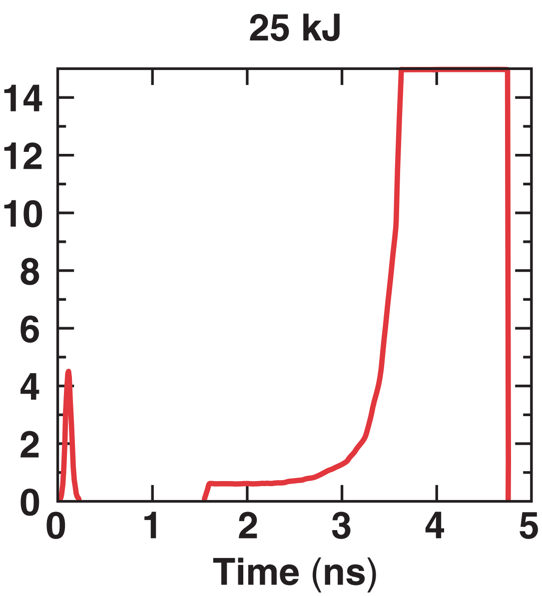

Maximum ρR	3 g/cm^2
α	0.7
V_i	1.7×10^7 cm/s
IFAR	18

Maximum ρR	1.9 g/cm^2
α	0.7
V_i	1.7×10^7 cm/s
IFAR	18

Maximum ρR	0.78 g/cm^2
α	1.0
V_i	2.6×10^7 cm/s
IFAR	30

Low-adiabat implosions are driven by RX laser pulses.

TC7586

Summary/Conclusions

Scaling laws relating stagnation and in-flight hydrodynamic variables are derived for the design of direct-drive ICF targets

FSC

UR LLE

- Such scaling laws can be used to optimize direct-drive target design.
- Scaling laws relating stagnation and in-flight variables are derived for hydrodynamic variables relevant to conventional and fast-ignition ICF
  - hydrodynamic efficiency and target gain
  - stagnation aspect ratio, shell density, and areal density
  - hot-spot areal density, temperature, and pressure
- Based on such scaling laws, fast-ignition targets require low-velocity, low-adiabat implosions